RESEARCH ARTICLE

Dynamic Behavior of Cu–Water and Al_2O_3–Water Nanofluids in a Thermally Radiative MHD Flow Over a Porous Channel

Anumolu Anupama[1], U. Venkata Kalyani[2], G. Venkata Ramana Reddy[3], Charankumar Ganteda[4], Vediyappan Govindan[5], Ghulam Rasool[6] and Muhammad Ijaz Khan[6,*]

[1] Department of Basic Engineering, DVR & Dr. HS MIC College of Technology Kanchikacherla, Andhra Pradesh 521180, India
[2] Department of Mathematics and Statistics, Vignan's Foundation for Science, Technology and Research, Andhra Pradesh, India
[3] Department of Integrated Research Discovery, Koneru Lakshmaiah Education Foundation, Vaddeswaram 522302, India
[4] Department of Mathematics, Koneru Lakshmaiah Education Foundation, Vaddeswaram 522302, India
[5] Department of Mathematics, Hindustan Institute of Technology and Science, Chennai, India
[6] Department of Mechanical Engineering, College of Engineering, Prince Mohammad Bin Fahd University, Saudi Arabia

Abstract

This study describes convective temperature and mass transport in a magnetohydrodynamic nanofluid moving via an absorbing channel stretched across an extensive region while being influenced by a securing region. The analytical framework incorporates a multitude of factors including heat generation, thermal radiation effects, viscous dissipation, and chemical reaction implications. The influences of porosity, warm production, thermal emission, attractive fields, sticky indulgence, and substance reactions on the flow dynamics are absolutely expounded across a spectrum of governing parameters. Furthermore, it is posited that regulation can be applied to the nanoparticle volume segment at the boundary interface. Two specific varieties of nanofluids, specifically Copper-Water (Cu-H_2O) with Aluminium Oxide-Water (Al_2O_3-H_2O), are engaged in the scrutiny. The sensible challenge is mathematically articulated as approaches of nonlinear differential equations, which are subsequently resolved arithmetically employing the fourth-order Runge-Kutta procedure in sequence with the shooting approach. A proportional assessment of our findings with formerly published occasions in the scholarly prose reveals a significant degree of concordance.

Keywords: MHD, porous media, thermal radiation, skin-friction, eckert number.

Submitted: 22 June 2025
Accepted: 08 July 2025
Published: 20 August 2025

Vol. 1, **No.** 1, 2025.
10.62762/IJTSSE.2025.532667

***Corresponding author:**
✉ Muhammad Ijaz Khan
2106391391@pku.edu.cn

Citation
Anupama, A., Kalyani, U. V., Reddy, G. V. R., Ganteda, C., Govindan, V., Rasool, G., & Khan, M. I. (2025). Dynamic Behavior of Cu–Water and Al_2O_3–Water Nanofluids in a Thermally Radiative MHD Flow Over a Porous Channel. *International Journal of Thermo-Fluid Systems and Sustainable Energy*, 1(1), 3–15.

1 Introduction

In contemporary scholarly discourse, significant emphasis has been placed on the investigation of nanofluids owing to their superior thermal attributes in comparison to traditional fluids. Nanofluids represent an innovative category of fluids comprising nanoparticles suspended within a base fluid. They have surfaced as a viable option for a myriad of industrial applications owing to their exceptional warm transport possessions. The phenomena of borderline sheet run in addition temperature transport over expanding outsides are integral to several production processes, which encompass polymer sheet extrusion, annealing, crystal growth processes, metal spinning, and hot rolling. Heat exchangers, where improved heat transfer due to nanofluid properties can lead to more compact and efficient designs; Cooling systems in electronics or automotive industries, where enhanced thermal conductivity and flow control are critical; Renewable energy systems, such as solar collectors, where nanofluid behavior under varying thermal conditions could improve energy capture and conversion efficiency. By clearly connecting the outcomes of our analysis to these engineering systems, we aim to bridge the gap between theoretical modeling and applied science, thereby making the findings more impactful for both academic and industrial audiences. Crane [1] was instrumental in initiating the exploration of flow dynamics past a stretching plate. Subsequently, a multitude of researchers have probed the flow with temperature transport descriptions of diverse fluids on extending faces. Khan et al. [2] conducted an examination of the borderline sheet flow of a nanofluid traversing a extending page. Abd El-Aziz [3] explored the thermal-dispersal plus dispersal-thermo properties on the joint temperature with mass allocation singularities linked with hydromagnetic three-dimensional allowed convection completed a penetrable widening exterior in combination through energy. Hady et al. [4] explored the guidance of emission on the sticky flow of a nanofluid and the associated temperature transport over a nonlinearly expanding page. Bachok et al. [5] analyzed the unstable borderline-sheet flow and temperature transport dynamics of a nanofluid throughout a absorbent extending/lessening piece. Rohni et al. [6] assessed the stream and temperature transport characteristics over an unstable dropping page with drag in a nanofluid utilizing Buongiorno's prototype. Buongiorno [7] proposed a two-component shape for the convective moving phenomena occurring in nanofluids. Sandhya et al. [8] examined the consequences of heat with dimension transfer on magnetohydrodynamic flow past an oriented permeable sheet in the context of a substance outcome. Murthy et al. [9] analyzed the implications of thick intemperance within a non-Darcy natural convection regime. Motsa [10] introduced a novel spectral relaxation technique for the analysis of resemblance changing nonlinear borderline sheet flow systems. Gladys et al. [11] assessed the influence of adjustable thickness and current conduction on the dynamics of non-Newtonian nanofluid flow preceding an rushing perpendicular shield. Vijaya et al. [12] scrutinized the magnetohydrodynamic movement of Casson liquid across a perpendicular permeable shield amidst the effects of emission, Soret, and chemical reactions. Oztop et al. [13] executed a mathematical investigation into real convection within moderately warmed quadrangular inclusions packed with nanofluids. Brinkman [14] formulated a model addressing the thickness of assembled postponements and explanations. Maxwell Garnett [15] articulated a theoretical framework for the coloration phenomena observed in metallic glasses and films. Abu-Nada [16] explored the applicability of nanofluids for the improvement of temperature transport in detached flows encountered in backward-facing steps. Hamad [17] derived a systematic liquid for the normal convection flow of a nanofluid throughout a linearly spreading layer under the influence of a attractive discipline. Kameswaran et al. [18] explored the hydromagnetic flow of nanofluids resulting from a spreading or falling slip, incorporating effects from sticky rakishness and substance responses. Grubka et al. [19] examined the temperature transport attributes associated with a endless extending outside exhibiting changing heat conditions. Patnaik et al. [20] conducted an investigation into the experimental investigation of Darcy indulgence variation of nanofluid with titanium dioxide (TiO_2) and copper (Cu) for the purpose of improving width implementation in a perpendicular area. Several different kinds of chemical reactions have been investigated by Dhange et al. [21] in order to determine how they influence the hydrodynamic parameters of scattering and peristaltic movement in couple-stress fluid. The influence of delamination on the changing aspects of bioconvective thixotropic liquid carrying small particles within the context of the Cattaneo-Christov model has been investigated and analyzed. Through the use of the Cattaneo-Christov model, Shamshuddin et al. [22] conducted an investigation into the Casson ternary

nanofluid integration under a variety of thermal and physical effects. Their focus was on investigating magnified heat transport in stretchable surfaces. Panda et al. [23] Computation of the movement of a hybrid nanofluid composed of Fe_3O_4 and $CoFe_2O_4$ in a expandable (Shrinkable) wedge through variable magnetised influence in addition temperature is shown.

According to Biswas et al. [24], an investigation was carried out into the effect of heat emission on the bioconvection flow of nano-enhanced level transition objects and oxytactic bacteria inside a vertical wavy porous cavity. Ganji et al. [25] observed that the presence of oxytactic microorganisms and a motivating attractive area led to the formation of a mixed bioconvection flow of water and calcium magnesium oxide. Rasool et al. [26] considered a solution for the MHD flow of nanofluids across a permeable medium, taking into account current emission, viscosity degeneration, and chemical reaction effects, as well as the transmission of heat and mass. Hussain et al. [27] studied the matched convection of Al_2O_3–Cu–water hybrid nanofluid in an undulating outlet with an inserted permanent cylinder as the medium, using Maxwell's method. Vinoth Kumar et al. [28] developed arithmetic explanations for the current and solutal transportation of Jeffrey liquid flow, which is governed by rotation, using the Keller–Box method. Dibaji et al. [29] examined a vertically inclined porous surface subjected to multi-walled carbon nanotubes injected with motor oil and titania nanoparticles. Obalalu et al. [30] investigated the thermal conductivity and dual solutions of hybrid nanofluids by comparing the Xue model with the Hamilton–Crosser mathematical model to better understand their relationship. Osman et al. [31] explored optimized slip movement of a viscous material in Ohmic boiling and its indulgence towards a curved moving surface. Zhai et al. [32] developed a novel catalytic micro-reactor model for hydrogen production using methane-steam reforming. Varun Kumar et al. [33] analyzed current circulation in a leaning porous fin using the generalized residual power series technique. Veclani et al. [34] investigated the impact of nano-graphene oxide functional groups on biodiesel production using DFT calculations. Khan et al. [35] examined Carreau liquid behavior in the context of Arrhenius activation energy and Brownian diffusion properties. Harby et al. [36] enhanced desalination performance in tropical environments through a combined cooling rotation process. Raju et al. [37] studied MHD flow and radiative heat/mass transfer in non-Newtonian nanomaterials under non-uniform heating. Virk et al. [38] developed anti-bacterial polymer nanocomposites in the presence of polysaccharide gum hydrogels. Raja et al. [39] demonstrated heat transfer in viscoelastic liquids towards a Riga surface using entropy concepts and neural networks (NN). Upendra et al. [40] incorporated enzyme-mimicking nanomaterials in micro-fluidic devices for biomedical applications. Puneeth et al. [41] investigated temperature and mass transfer in non-Newtonian nanoliquids influenced by motile gyrotactic microorganisms.

The investigation into convective temperature also dimension transference phenomena within nanofluids has recently gathered knowledge of academic interest. This investigation examines the detailed components of magneto-hydrodynamics (MHD), in combination with the temperature and mass transmission mechanisms present in the movement of nanofluids on a stretching surface, while factoring in aspects such as porous media, hydromagnetic forces, thermal energy making, current energy, glutinous indulgence, biochemical connections, and Soret phenomena. The mathematical result of the governing ordinary differential equations is performed utilizing the Runge-Kutta method in combination including BVP4C MATLAB 2021(a). The implementation of the Runge-Kutta strategy has illustrated impressive skills in managing a diverse set of difficulties in the sectors of fluid mechanics and thermal dynamics. This manuscript elucidates the intricacies of fluid dynamics and thermal transfer, while also highlighting the benefits associated with the employed solution technique.

1.1 Significance and objective

This investigation's implication is rooted in the exploration of the effects of emission and compound responses on the flow characteristics of magnetohydrodynamic (MHD) hybrid nanofluids traversing porous stretching surfaces, exemplified by Al_2O_3-Cu nanoparticles suspended in H_2O, particularly considering the influences of magnetic fields, current emission, in addition slip circumstances. This extensive examination of various liquid dynamics below multifaceted circumstances presents an innovative methodology and augments comprehension in domains such as magnetohydrodynamics and thermal management, with pragmatic implications for industries including

polymer administering, biomedical manufacturing, and biochemical manufacturing. The study forwards deficiencies in the succeeding domains:

- The investigation of these fluids under analogous conditions facilitates the identification of distinctive qualities and performances that significantly affect their operational presentation.
- The expanding page participates a crucial job in shaping the thickness, strength, with flexibility of materials. Moreover, the angle of inclination modifies convection undercurrents by modifying the interplay linking resistance and significance, rendering them critical influences in biofluid process, manufacturing production, and atmosphere submissions.
- Current emission provides a additional precise depiction of temperature transport mechanisms, specifically within elevated heat circumstances, such as those encountered in aerospace contexts.
- The incorporation of porous media enhances the superficial zone as concurrently calm down liquid flow in freezing techniques applicable to stratosphere and motorized manufacturing.
- The influence of attractive domains on non-Newtonian fluids may catalyze advancements in MHD presentations, including freezing organizations utilized in atomic devices and compelling preparation delivery systems.
- The Soret effect elucidates the correlation governing mass diffusion in hybrid nanofluids.
- Hybrid nanofluids composed of Al_2O_3 and Cu, with stream serving as the construct liquid, is utilized in refrigeration machineries with heat handover organizations due to its superior current possessions and effectiveness, which are requisite for contemporary advancements.

This study looks at these research questions.

- Various non-Newtonian hybrid nanofluids: how do they behave in an inclined expanding sheet?
- When the stretching surface is considered, how does this model fare?
- What influence do heat sources, radiation, and Soret factors have on the heat outline of the flow?
- What effect do the nanoparticles have on the flow of fluids?

2 Mathematical Formulation

The investigation pertains to the constant 2-dimensional borderline sheet flow of an in squeezable nanofluid that facilitates both thermal and mass transport throughout a porous expanding page. The source point for the approach is placed at the gap from which the area extends. Within this specified ordinate arrangement, the x-axis is aligned in the trend of the continuously extending appear. The y-axis is defined perpendicular to the level of the piece's surface. It is believed that the attractive pitch resulting from the flow is trivial in contrast to the magnetic field applied from outside. Moreover, it can be suggested that the magnetic field generated, along with the outside electric field and the field created by charge separation, hold little importance when compared to the magnetic field imposed from outside. Additionally, the influences of substance warming, nanoparticle collection, and sedimentation are intentionally excluded from the current analysis.

The fluid that is being examined is a nanofluid formed from a chiefly aqueous base that unites two varied categories of nanoparticles: Copper with Al_2O_3 nanoparticles. It is postulated that the found liquid with the nanoparticles exist in a condition of current equilibrium, devoid of any slip phenomena occurring concerning the two disparate phases. The qualities associated with the thermo-physical behavior of the nanofluid are specified in Table 1. Through the aforementioned premises, the leading borderline coating equations pertinent to the nanofluid flow, encompassing the continuity, momentum, energy, plus concentration pitches, alongside the effects of diffusion, radiation, thermal production, glutinous indulgence, in addition biochemical responses can be articulated in measurement procedure as delineated by Gladys et al. [11].

$$\frac{\partial u}{\partial x}+\frac{\partial v}{\partial y}=0 \tag{1}$$

$$u\frac{\partial u}{\partial x}+v\frac{\partial u}{\partial y}=\frac{\mu_{nf}}{\rho_{nf}}\frac{\partial^2 u}{\partial y^2}-\left\{\frac{\mu_{nf}}{\rho_{nf}}\frac{1}{K}+\frac{\sigma B_0^2}{\rho_{nf}}\right\}u \tag{2}$$

$$\begin{aligned}u\frac{\partial T}{\partial x}+v\frac{\partial T}{\partial y}&=\alpha_{nf}\frac{\partial^2 T}{\partial y^2}+\frac{Q_0}{(\rho c_p)_{nf}}(T-T_\infty)\\&+\frac{1}{(\rho c_p)_{nf}}\frac{16\sigma^* T_\infty^3}{3K^*}\frac{\partial^2 T}{\partial^2 y}+\frac{\mu_{nf}}{\left((\rho c_p)_{nf}\right.}\left(\frac{\partial u}{\partial y}\right)^2\end{aligned} \tag{3}$$

$$u\frac{\partial C}{\partial x}+v\frac{\partial C}{\partial y}=D_B\frac{\partial^2 C}{\partial y^2}+\frac{D_T}{T_\infty}\frac{\partial^2 T}{\partial y^2}-K_0\left(C-C_\infty\right) \quad (4)$$

The stipulations pertaining to the borderline restrictions for equations (1) - (4) are delineated like results:

$$\begin{cases} u=ax, v=0, T=T_w(x)=T_\infty+m\left(\frac{x}{\omega}\right)^2, \\ C=C_w(x)=C_\infty+n\left(\frac{x}{\omega}\right)^2 \text{ at } y=0 \\ \qquad u\to 0, T\to T_\infty, C\to C_\infty \text{ as } y\to\infty \end{cases} \quad (5)$$

where n, m and a are constants, $a > 0$ and ω is the attribute duration. u and v symbolize the speeds in x and y guidance, correspondingly. The possessions of the nanofluid, containing active viscosity, extent, current organise, particular warm volume, and current diffusivity are indicated by $\mu_{nf}, \rho_{nf}, k_{nf}, (\rho C_p)_{nf}$ and α_{nf} correspondingly. T and C are the heat and concentration, Q_0 is the heat source, D_B is the Brownian motion, K_0 is the chemical reaction, T_∞ and C_∞ are the ambient heat and absorption individually.

Here q_r is the emission heat flux [12] specified through

$$q_r=-\frac{4\sigma^*}{3K^*}\frac{\partial T^4}{\partial y} \quad (6)$$

where σ^* is the Stefen-Boltzmann continuous and K^* is the Rosseland average concentration constant. The heat alternative T^4 is increased in a Taylor series development sheet. Avoiding greater sequence relationship with increasing T^4 around T_∞ we obtain, $T^4 \cong 4T_\infty^3 T-3T_\infty^4$.

The efficient active thickness of the nanofluid was given by Brinkman [14] as

$$\mu_{nf}=\frac{\mu_f}{(1-\phi)^{2.5}} \quad (7)$$

Somewhere ϕ with μ_f are illustrate the nanoparticle constant quantity division and the vigorous viscosity pertaining to the source liquid, respectively. In equations (1) through (4), the thermal condenser of the nanofluid with the warm air conduction of nanofluids, specifically constrained to sphere-shaped nanoparticles, are estimated utilizing the Maxwell-Garnett exhibit (refer to Maxwell Garnett [15]).

$$\begin{gathered} (\rho c_p)_{nf}=(1-\phi)(\rho c_p)_f+\phi(\rho c_p)_s, \\ \rho_{nf}=(1-\phi)\rho_f+\phi\rho_s, v_{nf}=\frac{\mu_{nf}}{\rho_{nf}}, \\ \alpha_{nf}=\frac{k_{nf}}{(\rho c_p)_{nf}}, k_{nf}=k_f\left[\frac{(k_s+k_f)-2\phi(k_f-k_s)}{(k_s+k_f)+\phi(k_f-k_s)}\right], \end{gathered} \quad (8)$$

where $v_{nf}, \rho_{nf}, (\rho c_p)_{nf}, k_{nf}, k_f, k_s, \rho_s, (\rho c_p)_f, (\rho c_p)_s$ are the kinematic stickiness of nanofluids, the electrical conductivity characteristics, the specific heat capacity of the nanofluid, the current transmission exhibited by the nanofluid, the current transmission pertaining to the base liquid, the current conductivity relevant to the hard constituents, the concentration associated with the hard constituents, the illness capability of the base melted, with the actual heat ability attributed to nanoparticles, correspondingly.

The stability equation (1) is convinced by beginning a flow relation $\psi(x, y)$ then:

$$u=\frac{\partial\psi}{\partial y}, v=-\frac{\partial\psi}{\partial x}. \quad (9)$$

Introducing the following dimensionless variables,

$$\begin{gathered} \psi=[av_f]^{\frac{1}{2}}xf(\eta), u=axf'(\eta), v=-(av_f)f(\eta), \\ \theta(\eta)=\frac{T-T_\infty}{T_w-T_\infty}, \varphi(\eta)=\frac{C-C_\infty}{C_w-C_\infty}, \eta=\left[\frac{a}{v_f}\right]^{\frac{1}{2}}y \end{gathered} \quad (10)$$

where η is the resemblance variable, $f(\eta)$ is the non-dimension stream function, $\theta(\eta)$ is the non-dimension heat in addition $\varphi(\eta)$ is the non-dimension absorption. By weaving together equations (6), (7), (9), in addition (10), the foundational equations (2), (3), and (4), alongside the borderline environment (5), evolve into the subsequent two-point border line appreciate conundrum:

$$f'''+B_1\left[ff''-f'^2-\frac{1}{B_2}Mf'\right]-K_1f'=0, \quad (11)$$

$$\left(1+\frac{4R}{3}\right)\theta''+Pr\frac{k_f}{k_{nf}}B_3\left[f\theta'-2f'\theta+Q\theta+\frac{E_c}{B_4}f''^2\right]=0 \quad (12)$$

$$\varphi''+Sc\left(f\varphi'-2f'\varphi+Kr\varphi\right)+Sr\theta''=0 \quad (13)$$

topic to the border line specifications

$$\begin{gathered} f=0, f'=1, \theta=1, \varphi=1 \text{ at } \eta=0 \text{ and} \\ f'\to 0, \theta\to 0, \varphi\to 0 \text{ as } \eta\to\infty \end{gathered} \quad (14)$$

where primes suggest the procedure of taking the derivative $\eta, \alpha_f = k_f/(\rho c_p)_f$ also $v_f = \mu_f/\rho_f$ are the thermal diffusivity and kinetic thickness of the basis liquid, correspondingly. Other non-dimensional constraints showing in equations (11) to (14) are $M, K_1, R, \Pr, Q, E_c, Sc, Kr$ and Sr symbolize the attractive restriction the permeable medium restriction the thermal energy constraint the Prandtl number the temperature production restriction the Eckert number the Schmidt number the climbed biochemical response restriction and the Soret number. We can describe this components using math as results

$$\begin{gathered} M = \frac{\sigma B_0^2}{a\rho_f}, K_1 = \frac{v_f}{ak}, R = \frac{4\sigma^* T_\infty^3}{k^* k_{nf}}, Sc = \frac{v_f}{D}, \\ Pr = \frac{v_f(\rho c_p)_f}{k_f}, Q = \frac{Q_0}{a(\rho c_p)_{nf}}, Kr = \frac{K_0}{a}, \\ E_c = \frac{u_w^2}{(T_w - T_\infty)(c_p)_f}, Sr = \frac{D_1(T_w - T_\infty)}{D(C_w - C_\infty)}. \end{gathered} \tag{15}$$

The nanoparticle volume fraction ϕ_1 also ϕ_2 are described as

$$\begin{gathered} B_1 = (1-\phi)^{2.5}\left[1 - \phi + \phi\left(\frac{\rho_s}{\rho_f}\right)\right], B_2 = 1 - \phi + \phi\frac{(\rho_s)}{(\rho_f)}, \\ B_3 = 1 - \phi + \phi\frac{(\rho c_p)_s}{(\rho c_p)_f}, B_4 = (1-\phi)^{2.5}\left[1 - \phi + \phi\frac{(\rho c_p)_s}{(\rho c_p)_f}\right]. \end{gathered} \tag{16}$$

3 Skin friction, heat and mass transfer coefficients

The important measurement in obtaining is the skin resistance constant C_f, the local Nusselt number Nu_x and the local Sherwood number Sh_x illustrate the appear draggle, Proportions of temperature with magnitude transport at the wall. The pressure from cropping at the wall's exterior.τ_w is defined as

$$\tau_w = -\mu_{nf}\left(\frac{\partial u}{\partial y}\right)_{y=0} = -\frac{1}{(1-\phi)^{2.5}}\rho_f\sqrt{v_f a^3}\, x f''(0), \tag{17}$$

where μ_{nf} is the constant of thickness. The skin friction measurement is achieved as

$$C_{fx} = \frac{2\tau_w}{\rho_f U_w^2}, \tag{18}$$

also get through equation (17) in (18) we found

$$0.5(1-\phi)^{2.5} C_{fx} = -Re_x^{-\frac{1}{2}} f''(0). \tag{19}$$

The rate of temperature transport at the wall's exterior is defined as

$$q_w = -k_{nf}\left(\frac{\partial T}{\partial y}\right)_{y=0} = -k_{nf}\frac{(T_w - T_\infty)}{x}\sqrt{\frac{U_w x}{v_f}}\theta'(0), \tag{20}$$

where k_{nf} is the current conduction of the nanofluid. The local Nusselt number is explained as

$$Nu_x = \frac{x q_w}{k_f (T_w - T_\infty)}. \tag{21}$$

Applying equation (20) in equation (21), the non dimension wall temperature transport rate is taken as

$$\left(\frac{k_f}{k_{nf}}\right) Nu_x = -Re_x^{0.5}\theta'(0). \tag{22}$$

The amount of mass flowing at the wall surface is explained as

$$q_m = -D\left(\frac{\partial C}{\partial y}\right)_{y=0} = -DQ\left(\frac{x}{\omega}\right)^2\sqrt{\frac{a}{v_f}}\varphi'(0), \tag{23}$$

also the local Sherwood number is attained so

$$Sh_x = \frac{x q_m}{D(C_w - C_\infty)}. \tag{24}$$

The non dimension wall mass transport rate from (23) and (24) is obtained as

$$Sh_x = -Re_x^{\frac{1}{2}}\varphi'(0) \tag{25}$$

where Re_x symbolizes the local Reynolds number also is explained so

$$Re_x = \frac{x u_w}{v_f} \tag{26}$$

4 Technique of Result

The analytical resolution of the modified governing ordinary differential equations (ODEs) is executed through the integration of the classical fourth-order Runge-Kutta scheme alongside the bvp4c solver in MATLAB 2021a. Initially, the ensemble of higher-order nonlinear ODEs is reformulated interested in a method of first-order equations to render it amenable to mathematical analysis. The Runge-Kutta method is utilized to produce precise initial estimates for the solution profiles, which are integral to guaranteeing the stability and convergence of the boundary value problem (BVP) solver. Subsequently, the MATLAB function bvp4c—a robust and extensively employed boundary value problem solver grounded in a collocation method with adaptive mesh refinement—is deployed to derive the ultimate numerical solutions. This methodology assures elevated accuracy and computational efficiency when addressing intricate coupled nonlinear systems subject to boundary conditions at two distinct points (e.g., at the surface and as $\eta \to \infty$).

5 Results and Discussion

The nonlinear borderline cost badly-behaved delineated by equations (12) to (14), in conjunction with the boundary conditions specified in (15) and (16), is not amenable to an analytical solution; thus, these equations are addressed through numerical methods employing the fourth-order Runge-Kutta procedure combined through the shooting method aimed at Cu-water and water-based nanofluids, where water serves as the primary liquid (i.e., maintaining a continuous Prandtl number). The thermophysical characteristics of the nanofluids incorporated in the arithmetic models are presented in Table 1. We need to do a lot of estimates to obtain the speed hotness and absorption outlines. We also glimpsed at skin friction local Nusselt number and local Sherwood number for different basic restrictions then $\phi, M, K_1, R, Pr, Sc, Q, E_c, Kr$ and Sr. In Table 2 The text supports estimated values for the skin friction constant temperature allocation at the external with dimension transport costs at several flow circumstances. The L and Nt in the diagrams correspond to the major Lth and Ntth rehearsal complicated to make joining solutions. It is experiential that the growing values of Sr growing Sherwood growths in case of Cu-water but the converse growth is studied including Al_2O_3-water. Furthermore growing the values of Sc promote the Sherwood numbers for composed cases of nanofluids whereas mounting in heat generation parameter Q be probable to decrease the temperature carriage rate for organized nanofluids. The table too specifies that exterior mass bearing charges rises with upward in the rates of the chemical reaction parameter Kr as can be experimental from Table 2.

Table 1. Thermal physical properties.

Material Possessions	Base fluid (H_2O)	Copper (Cu)	Alumina (Al_2O_3)
C_p (J/kgK)	4179	385	765
ρ (Kg/m^3)	997.1	8933	3970
k (W/mK)	0.613	401	40

We now elucidate that the augmentation in the skin friction coefficient in relation to specific parameters (e.g., magnetic field intensity or nanoparticle volumetric fraction) signifies an enhanced resistance at the boundary layer, attributable to intensified Lorentz or viscous forces. Correspondingly, the elevation in the Nusselt number concomitant through

Table 2. Relationship of the SRM explanations for $f''(0), -\theta'(0)$, and $-\varphi'(0)$ for separate values of Sr, Sc, Q and $Kr \cdot \ \phi = 0.1, E_c = 1, M = 0.5, Sc = 1, Q = 0.02, \Pr = 7, K_1 = 1, Kr = 0.08, Sr = 0.2$.

	Cu + water			Al_2O_3 + water		
	$\phi = 0.1, E_c = 1$		$R = 1.5, Pr = 7$		$K_1 = 1.25, M = 0.5$	
Sr	$f''(0)$	$-\theta'(0)$	$-\varphi'(0)$	$f''(0)$	$-\theta'(0)$	$-\varphi'(0)$
0.0	1.662604	0.262148	1.202677	1.543301	0.387825	1.231629
0.1	1.662604	0.262148	1.203733	1.543301	0.387825	1.223235
0.3	1.662604	0.262148	1.205845	1.543301	0.387825	1.206450
0.4	1.662604	0.262148	1.206901	1.543301	0.387825	1.198053
Sc						
0.6	1.662604	0.262148	1.204789	1.543301	0.387825	1.214843
0.7	1.662604	0.262148	1.574980	1.543301	0.387825	1.587532
0.8	1.662604	0.262148	1.887968	1.543301	0.387825	1.901664
0.9	1.662604	0.262148	2.163376	1.543301	0.387825	2.177699
Kr						
0.6	1.662604	0.262148	1.140069	1.543301	0.387825	1.155418
0.7	1.662604	0.262148	1.219003	1.543301	0.387825	1.228160
0.8	1.662604	0.262148	1.438686	1.543301	0.387825	1.439334
0.9	1.662604	0.262148	1.642761	1.543301	0.387825	1.639504

an growth in thermal conductivity or nanoparticle concentration denotes an improvement in heat transmission, which arises from the improved current energy diffusion characteristics of the hybrid nanofluid.

Moreover, we have incorporated a paragraph that addresses the practical implications of our findings. These results imply that by meticulously optimizing nanoparticle combinations and flow parameters, the thermal efficiency of systems such as cooling apparatuses, solar thermal collectors, or microfluidic heat exchangers can be significantly enhanced. This understanding holds considerable importance for the design of sophisticated thermal management technologies.

The properties of physical factors on several liquid energetic measures are shown in Symbols 1 - 11. Figure 1 illustrates how the attractive consideration M affects the speed describe of the nanofluids Cu-water and Al_2O_3-water. The nanofluid speed outlines of Cu-water and Al_2O_3-water decrease as the attractive factor M rises. This is because the request of a oblique attractive pitch to a fluid that conducts electricity causes a retarding Lorenz power, which reduces liquid motion in the borderline coating besides so reduces speed at the expenditure of raising heat plus solute concentration. Figure 2 depicts how the velocity of cu-water and Al_2O_3-water nanofluids is influenced by the porous medium constraint K_1. The speed outlines of both nanofluids are decreased when the porous medium parameter K_1 is increased. According to the

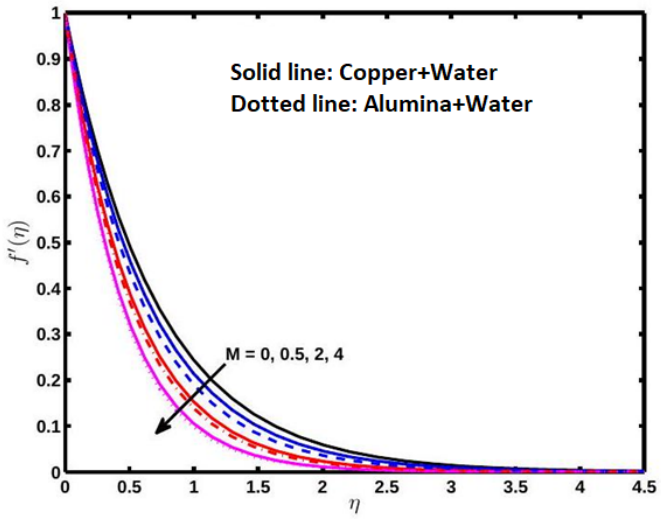

Figure 1. Impact of attractive constraint M on the speed outlines.

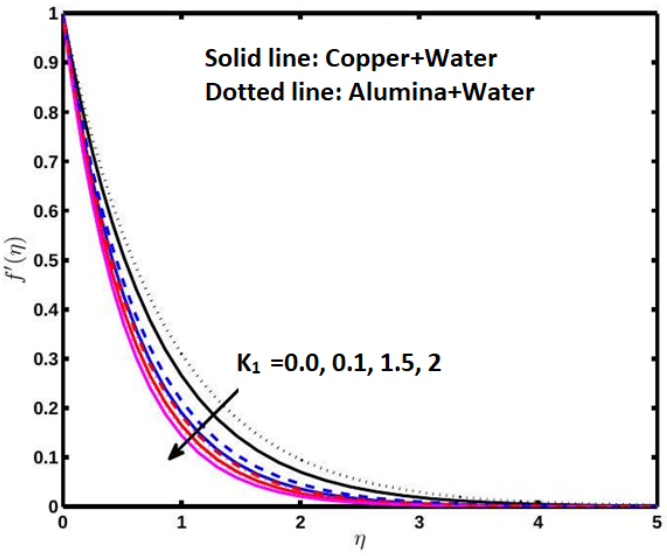

Figure 2. Impact of the porous medium parameter K_1 on the speed outlines.

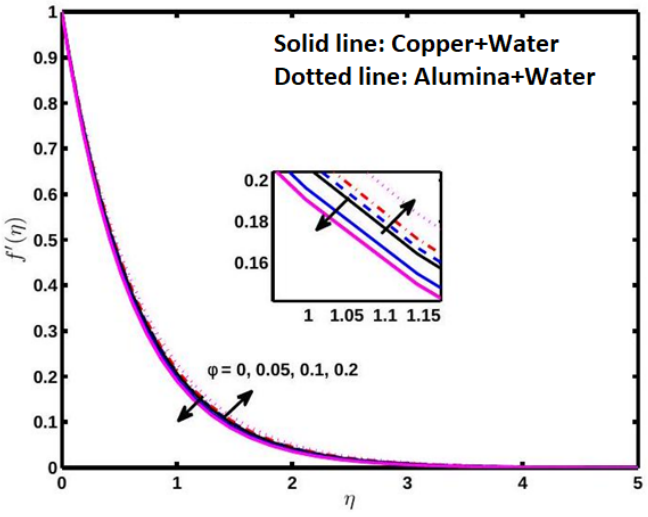

Figure 3. Impact of numerous nanoparticle values fraction ϕ on speed outlines.

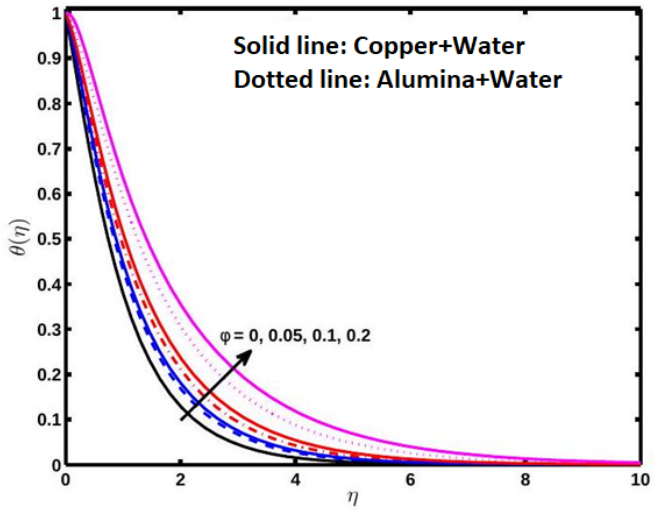

Figure 4. Appearance of different nanoparticle values division ϕ on heat outlines.

Figure 2, Al_2O_3-water nanofluid has a greater velocity profile than Cu-water nanofluid.

In the cases of a Cu-liquid nanofluid with an Al_2O_3-water nanofluid, Figures 3, 4 and 5 exhibit the influences of the nanoparticle degree division arranged the speed, heat, and absorption profiles, correspondingly. The Cu-water nanofluid velocity drops whereas the Al_2O_3-water nanofluid speed rises as the nanoparticle volume fraction rises. Figure 4 makes it clear that When you add more nanoparticles to a liquid it makes the liquid behavior temperature improved. This enhancement indicates to a thicker thermal border line cover. As indicated in Figure 1, the heat sketch expands as the values of nanoparticle volume segment growth. Since Cu-water exhibits excellent thermal conductivity and energy transfer performance, it is also noted that the heat allocation in a Cu-water nanofluid is greater than that in an Al_2O_3-water nanofluid. As the volume percentage of nanoparticles rises, the Al_2O_3-water nanofluid concentration profile falls, but it still resembles that of Cu-water nanofluid, as illustrated in Figure 5.

Figure 6 explains the guidance of temperature production factor Q on the heat designate in the project of Cu-water with Al_2O_3-water nanofluids. We noticed that the heat goes up for both types of nanofluids while the heat generation factor Q increases. It discovered that the heat of Cu-water is superior than of Al_2O_3-water nanofluids. Raising the temperature, making value known as Q boosts the thermal conduction of the nanofluid and makes the

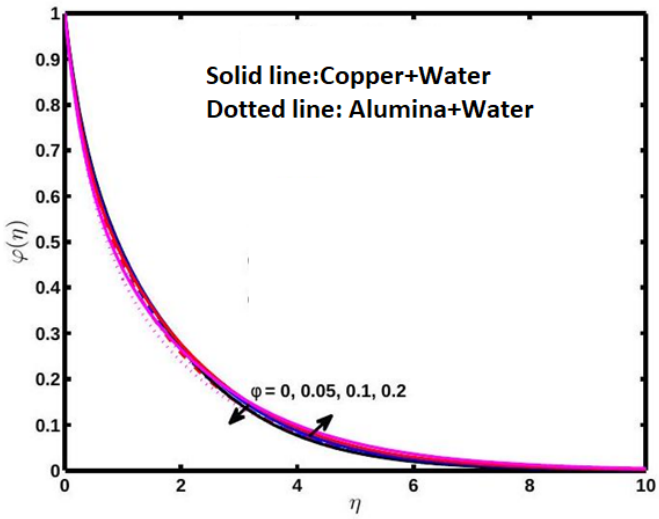

Figure 5. Appearance of different nanoparticle values division ϕ on the concentration outlines.

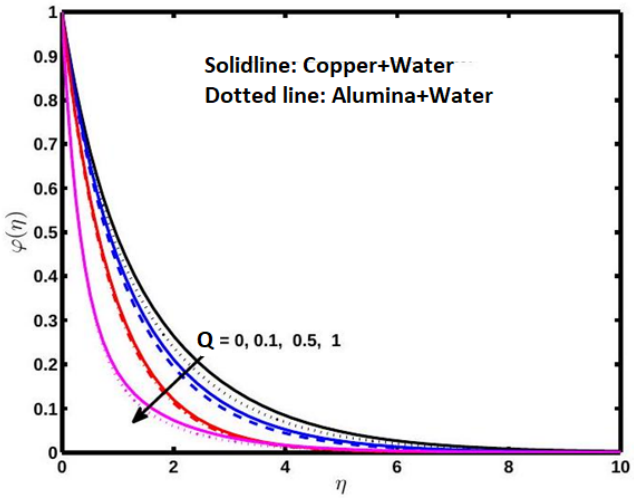

Figure 6. Effect of heat generation parameter Q on the heat outlines.

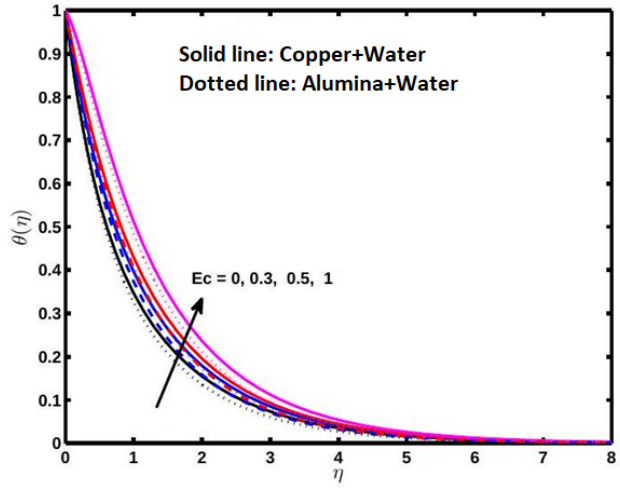

Figure 7. Impact of viscous dissipation constraint E_c on the heat profiles.

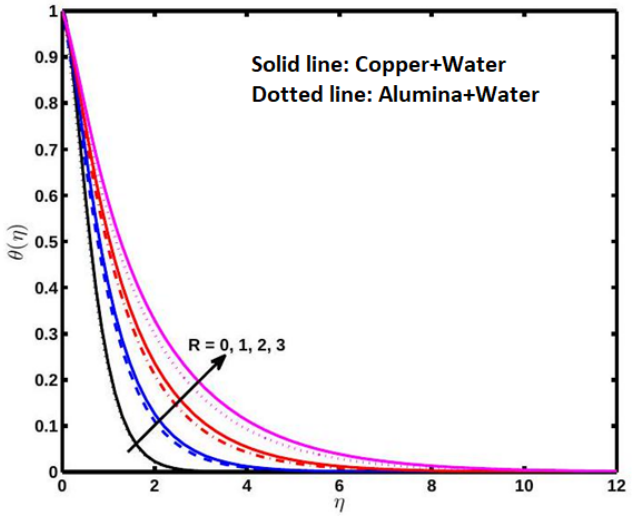

Figure 8. Impact of thermal emission constraint R on the heat outlines.

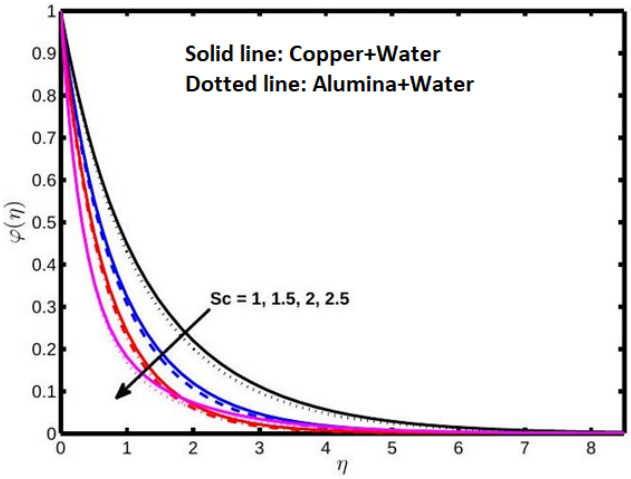

Figure 9. Impact of the Schmidt number Sc on absorption outlines.

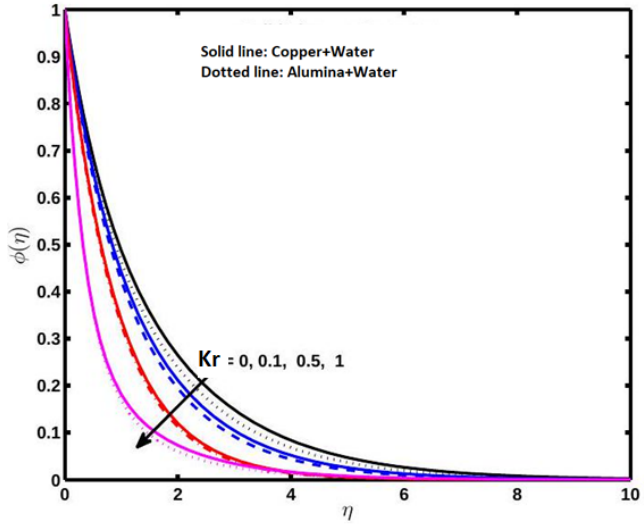

Figure 10. Impression of the compound response issue Kr on the absorption outlines.

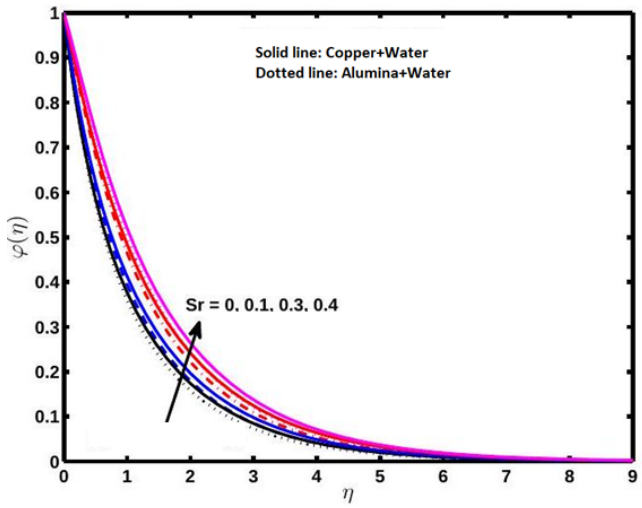

Figure 11. Impact of the Soret number Sr on meditation outlines.

current border line sheet marked.

Figure 7 depicts how the viscous indulgence factor E_c affects the heat outline for the nanofluids Al_2O_3 and Cu. With an increase in E_c values, it is seen that both nanofluids' temperature profiles rise; this suggests that an growth in E_c influences the infection spreading. This is because the liquid region stores the energy after it dissipates due to viscosity and elastic deformation. Cu-water nanofluid exhibits a greater temperature profile than Al_2O_3-water nanofluid, it has been observed.

Figure 8 depicts how the thermal emission factor R affects both nanofluids' heat profiles. Cu-water and Al_2O_3-water nanofluids have higher heat profiles when the thermal emission Factor R is increased. We found that Cu-water nanofluids exhibit larger temperature increases than Al_2O_3-water nanofluids. The stiffening of the thermal borderline sheet is caused by the thermal radiation parameter R. As a result, the system is cooled and the nanofluids can discharge the temperature resources from the flow zone. This is accurate since a larger Rosseland approximation causes a larger heat profile.

Figure 9 shows how the Schmidt number Sc effects the attention outline for nanofluids made of Cu and Al_2O_3. Both cases of nanofluids have a lower solutal concentration profile when Sc values are increased. Cu water nanofluid's concentration profile is seen to increase more than AI_2O_3-water nanofluid's.

Figures 10 and 11 demonstrate the impact of two parameters, namely the Soret number Sr and the biochemical response restriction Kr, on the concentration outlines for the Cu-water and Al_2O_3-water nanofluids, respectively. In contrast, the chemical reaction parameter's result on the nanofluid heat and speed describes in the two cases of the nanofluids does not vary substantially with swelling values of the scale biological response parameter. Al_2O_3-water nanofluid's solutal concentration profiles in Figure 10 are relatively different from those of Cu-water nanofluid's. The solutal absorption borderline sheet width of together cases of nanofluids grows as the Soret number Sr increases, as shown in Figure 11. We discovered that Al_2O_3-water nanofluid has lower solutal concentration outlines increase than Cu-water nanofluid.

6 Conclusion

We have assessed the impacts of heat generation, substance response, sticky intemperance, thermal radiation, afterward steady MHD borderline sheet flow in nanofluids over a permeable owing to a enlarging appear subjected to a attractive area. The following are some conclusions that can be taken from the numerical simulations:

- Cu-water nanofluid's velocity profile decreases with increasing nanoparticle volume segment, whereas Al_2O_3-water nanofluid's speed profile growths with increasing nanoparticle volume fraction. Both nanofluid's velocity profiles also decrease with encouraging attractive with permeable moderate restrictions.
- The concentration of Al_2O_3-water nanofluids decreases with growing values of the nanoparticle volume segment, whereas the heat outline of together nanofluids rises through improving values of the nanoparticle volume segment. The concentration of Cu-water nanofluids exhibits the opposite movement with swelling values of the nanoparticle size division.
- In both cases, the concentration describe of the nanofluids falls as the standards of the substance response issue and Schmidt number rise, whereas the Soret number exhibits the reverse tendency as its values rises.
- The thickness of the thermal borderline sheet in both nanofluids gets smaller while there are more nanoparticles when thermal radioactivity is current in permeable materials and due to the effects of depth in the flow.
- In all-purpose, the Al_2O_3-water nanofluid

illustrations a thicker speed coating at the shield than a Cu-water nanofluids; Al_2O_3-water nanofluid exhibitions extreme current with concentration borderline coat than a Cu-water nanofluid.

Nomenclature

u, v	Velocity components
x, y	Coordinate axes
T_w	Stretching surface temperature (K)
T_∞	Ambient fluid temperature (K)
C_∞	Ambient fluid concentration (g/L)
μ	Dynamic viscosity (N.s/m^2)
γ	Kinetic viscosity (m^2/s) [L^{2}T^{-1}]
C_f	Skin friction (Pa)
P_r	Prandtl number
Re_b	Reynold's number
M	Magnetic parameter (T)
R	Radiation parameter
Q	Heat generation parameter (J/s)
K	Porous parameter
σ^*	Stefan-Boltzman constant
τ_w	Stress (N/m^2)
q_w	Wall heat flux (W/m^2)
q_m	Mass heat flux (W/m^2)
α	Thermal diffusivity [MLT^{-3}K^{-1}]
θ	Dimensionless temperature
$\emptyset$	Dimensionless concentration
f'	Dimensionless fluid velocity
Ψ	Stream function (m^2/s)
B_0	Magnetic field strength [L^{-1}A]
k	Thermal constant (Wm^{-1}K^{-1})
Nu_x	Nusselt number
Sh_x	Sherwood number

Data Availability Statement

Data will be made available on request.

Funding

This work was supported without any funding.

Conflicts of Interest

The authors declare no conflicts of interest.

Ethical Approval and Consent to Participate

Not applicable.

References

[1] Crane, L. J. (1970). Flow past a stretching plate. *Zeitschrift für angewandte Mathematik und Physik ZAMP, 21*(4), 645-647. [Crossref]

[2] Khan, W. A., & Pop, I. (2010). Boundary-layer flow of a nanofluid past a stretching sheet. *International journal of heat and mass transfer, 53*(11-12), 2477-2483. [Crossref]

[3] Abd El-Aziz, M. (2008). Thermal-diffusion and diffusion-thermo effects on combined heat and mass transfer by hydromagnetic three-dimensional free convection over a permeable stretching surface with radiation. *Physics Letters A, 372*(3), 263-272. [Crossref]

[4] Hady, F. M., Ibrahim, F. S., Abdel-Gaied, S. M., & Eid, M. R. (2012). Radiation effect on viscous flow of a nanofluid and heat transfer over a nonlinearly stretching sheet. *Nanoscale Research Letters, 7*(1), 229. [Crossref]

[5] Bachok, N., Ishak, A., & Pop, I. (2012). Unsteady boundary-layer flow and heat transfer of a nanofluid over a permeable stretching/shrinking sheet. *International Journal of Heat and Mass Transfer, 55*(7-8), 2102-2109. [Crossref]

[6] Rohni, A. M., Ahmad, S., & Pop, I. (2012). Flow and heat transfer over an unsteady shrinking sheet with suction in nanofluids. *International Journal of Heat and Mass Transfer, 55*(7-8), 1888-1895. [Crossref]

[7] Buongiorno, J. (2006). Convective transport in nanofluids. [Crossref]

[8] Sandhya, A., Ramana Reddy, G. V., & Deekshitulu, V. S. R. G. (2020). Heat and mass transfer effects on MHD flow past an inclined porous plate in the presence of chemical reaction. *International Journal of Applied Mechanics and Engineering, 25*(3). [Crossref]

[9] Murthy, P. V. S. N., & Singh, P. (1997). Effect of viscous dissipation on a non-Darcy natural convection regime. *International journal of heat and mass transfer, 40*(6), 1251-1260. [Crossref]

[10] Motsa, S. S. (2014). A new spectral relaxation method for similarity variable nonlinear boundary layer flow systems. *Chemical Engineering Communications, 201*(2), 241-256. [Crossref]

[11] Gladys, T., & Reddy, G. R. (2022). Contributions of variable viscosity and thermal conductivity on the dynamics of non-Newtonian nanofluids flow past an accelerating vertical plate. *Partial Diff. Eq. Appl. Math, 5*, 100264. [Crossref]

[12] Vijaya, K., & Reddy, G. V. R. (2019). Magnetohydrodynamic Casson fluid flow over a vertical porous plate in the presence of radiation, Soret and chemical reaction effects. *Journal of Nanofluids, 8*(6), 1240-1248. [Crossref]

[13] Oztop, H. F., & Abu-Nada, E. (2008). Numerical study of natural convection in partially heated rectangular enclosures filled with nanofluids. *International journal*

of heat and fluid flow, 29(5), 1326-1336. [Crossref]

[14] Brinkman, H. C. (1952). The viscosity of concentrated suspensions and solutions. *Journal of chemical physics, 20*(4), 571-571. [Crossref]

[15] Maxwell-Garnett, J. C. (1904). XII. Colours in metal glasses and in metallic films. *Philosophical Transactions of the Royal Society of London. Series A, Containing Papers of a Mathematical or Physical Character, 203*(359-371), 385-420. [Crossref]

[16] Abu-Nada, E. (2008). Application of nanofluids for heat transfer enhancement of separated flows encountered in a backward facing step. *International Journal of Heat and Fluid Flow, 29*(1), 242-249. [Crossref]

[17] Hamad, M. A. A. (2011). Analytical solution of natural convection flow of a nanofluid over a linearly stretching sheet in the presence of magnetic field. *International communications in heat and mass transfer, 38*(4), 487-492. [Crossref]

[18] Kameswaran, P. K., Narayana, M., Sibanda, P., & Murthy, P. V. S. N. (2012). Hydromagnetic nanofluid flow due to a stretching or shrinking sheet with viscous dissipation and chemical reaction effects. *International Journal of Heat and Mass Transfer, 55*(25-26), 7587-7595. [Crossref]

[19] Grubka, L. J., & Bobba, K. M. (1985). Heat transfer characteristics of a continuous stretching surface with variable temperature. *Journal of Heat Transfer, 107*(1), 248-250. [Crossref]

[20] Pattnaik, P. K., Shamshuddin, M. D., Mishra, S. R., & Panda, S. (2025). Exploring Darcy dissipation modulation of nanofluid with titanium dioxide (TiO2) and copper (Cu) for enhanced thermal performance in a vertical sheet. *Case Studies in Thermal Engineering, 68*, 105904. [Crossref]

[21] Dhange, M., Devi, C. U., Jamshed, W., Eid, M. R., Ramesh, K., Shamshuddin, M. D., ... & Batool, K. (2024). Studying the effect of various types of chemical reactions on hydrodynamic properties of dispersion and peristaltic flow of couple-stress fluid: Comprehensive examination. *Journal of Molecular Liquids, 409*, 125542. [Crossref]

[22] Shamshuddin, M. D., Panda, S., Salawu, S. O., Mishra, S. R., & Patil, V. S. (2025). Analysis of Casson ternary nanofluid integration under various thermal physical impacts with Cattaneo-Christov model: Exploring magnified heat transfer in stretchy surface. *International Journal of Hydrogen Energy, 101*, 450-460. [Crossref]

[23] Panda, S., Shamshuddin, M. D., Mishra, S. R., Khan, U., Ishak, A., Salawu, S. O., & Pattnaik, P. K. (2024). Computation of Fe3O4-CoFe2O4 hybrid nanofluid flow in stretchable (Shrinkable) wedge with Variant magnetized force and heat generation. *Engineering Science and Technology, an International Journal, 58*, 101839. [Crossref]

[24] Biswas, N., Mandal, D. K., Manna, N. K., & Benim, A. C. (2023). Enhanced energy and mass transport dynamics in a thermo-magneto-bioconvective porous system containing oxytactic bacteria and nanoparticles: cleaner energy application. *Energy, 263*, 125775. [Crossref]

[25] Ganji, D. D., Mahboobtosi, M., & Chari, F. N. (2025). Three-dimensional flow analysis of penta and ternary-hybrid nanofluids over an elongating sheet with thermal radiation and gyrotactic microorganisms. *Scientific Reports, 15*(1), 24396. [Crossref]

[26] Rasool, G., Shah, N. A., El-Zahar, E. R., & Wakif, A. (2025). Numerical investigation of EMHD nanofluid flows over a convectively heated riga pattern positioned horizontally in a Darcy-Forchheimer porous medium: Application of passive control strategy and generalized transfer laws. *Waves in Random and Complex Media, 35*(3), 6039-6058. [Crossref]

[27] Hussain, S., Jamal, M., Maatki, C., Ghachem, K., & Kolsi, L. (2021). MHD mixed convection of Al_2O_3–Cu–water hybrid nanofluid in a wavy channel with incorporated fixed cylinder. *Journal of Thermal Analysis and Calorimetry, 144*(6), 2219-2233. [Crossref]

[28] Vinoth Kumar, B., & Poornima, T. (2025). Analysis of Jeffrey fluid over a vertical porous plate in Keller box method. *Multiscale and Multidisciplinary Modeling, Experiments and Design, 8*(8), 1-18. [Crossref]

[29] Dibaji, A. S., Rashidi, A., Baniyaghoob, S., & Shahrabadi, A. (2022). Synthesizing CNT-TiO2 nanocomposite and experimental pore-scale displacement of crude oil during nanofluid flooding. *Petroleum Exploration and Development, 49*(6), 1430-1439. [Crossref]

[30] Obalalu, A. M., Shah, S. H. A. M., Darvesh, A., Khan, U., Ishak, A., Adegbite, P., ... & Galal, A. M. (2024). Insight into the Hamilton and Crosser model for ternary hybrid nanofluid flow over a Riga wedge with heterogeneous catalytic reaction. *The European Physical Journal Special Topics*, 1-22. [Crossref]

[31] Osman, S., Amidu, M. A., Afgan, I., & Addad, Y. (2024). Experimental study of boiling heat transfer of inclined down-ward facing heated curved wall under low flow and pressure conditions. *Applied Thermal Engineering, 236*, 121706. [Crossref]

[32] Zhai, X., Ding, S., Cheng, Y., Jin, Y., & Cheng, Y. (2010). CFD simulation with detailed chemistry of steam reforming of methane for hydrogen production in an integrated micro-reactor. *International Journal of Hydrogen Energy, 35*(11), 5383-5392. [Crossref]

[33] Varun Kumar, R. S., Sowmya, G., Jayaprakash, M. C., Prasannakumara, B. C., Khan, M. I., Guedri, K., ... & Galal, A. M. (2022). Assessment of thermal distribution through an inclined radiative-convective porous fin of concave profile using generalized residual power series method (GRPSM). *Scientific Reports, 12*(1), 13275. [Crossref]

[34] Veclani, D., Tolazzi, M., & Melchior, A. (2020). Molecular interpretation of pharmaceuticals' adsorption on carbon nanomaterials: theory meets experiments. *Processes, 8*(6), 642. [Crossref]

[35] Ijaz Khan, M., Qayyum, S., Nigar, M., Chu, Y. M., & Kadry, S. (2023). Dynamics of Arrhenius activation energy in flow of Carreau fluid subject to Brownian motion diffusion. *Numerical Methods for Partial Differential Equations, 39*(6), 4468-4488. [Crossref]

[36] Harby, K., Ali, E. S., & Almohammadi, K. M. (2021). A novel combined reverse osmosis and hybrid absorption desalination-cooling system to increase overall water recovery and energy efficiency. *Journal of Cleaner Production, 287*, 125014. [Crossref]

[37] Raju, C. S. K., Sandeep, N., & Malvandi, A. (2016). Free convective heat and mass transfer of MHD non-Newtonian nanofluids over a cone in the presence of non-uniform heat source/sink. *Journal of Molecular Liquids, 221*, 108-115. [Crossref]

[38] Virk, K., Sharma, K., Kapil, S., Kumar, V., Sharma, V., Pandey, S., & Kumar, V. (2022). Synthesis of gum acacia-silver nanoparticles based hydrogel composites and their comparative anti-bacterial activity. *Journal of Polymer Research, 29*(4), 118. [Crossref]

[39] Zahoor Raja, M. A., Shoaib, M., El-Zahar, E. R., Hussain, S., Li, Y. M., Khan, M. I., ... & Malik, M. Y. (2025). Heat transport in entropy-optimized flow of viscoelastic fluid due to Riga plate: analysis of artificial neural network. *Waves in Random and Complex Media, 35*(1), 1077-1096. [Crossref]

[40] Upendra Lambe, U. L., Minakshi, P., Basanti Brar, B. B., Madhusudan Guray, M. G., Ikbal, I., Koushlesh Ranjan, K. R., ... & Manimegalai, J. (2016). Nanodiagnostics: a new frontier for veterinary and medical sciences.

[41] Puneeth, V., Khan, M. I., Narayan, S. S., El-Zahar, E. R., & Guedri, K. (2025). The impact of the movement of the gyrotactic microorganisms on the heat and mass transfer characteristics of Casson nanofluid. *Waves in Random and Complex Media, 35*(2), 3852-3875. [Crossref]

Dr. Muhammad Ijaz Khan Received MS and PhD from Quaid-I-Azam University, Islamabad, Pakistan in the year 2016 and 2019 in Applied Mathematics for work in the field of CFD analysis, Flow Behavior and Numerical techniques (AI). Currently working as Assistant Professor in the Department of Mechanical Engineering, Prince Mohammad Bin Fahd University, P. O. Box, 1664, Al-Khobar 31952, Kingdom of Saudi Arabia. Contributed more than 50 research-level papers to many International journals. Research interests include Sensor Networks, Machine Learning, and Cloud computing, Flow Behavior, CFD analysis.